Research Article

Journal of Innate Immunity

J Innate Immun 2018;10:30–43
DOI: 10.1159/000480386

Received: May 2, 2017
Accepted after revision: August 13, 2017
Published online: October 17, 2017

Immunoregulation of Neutrophil Extracellular Trap Formation by Endothelial-Derived p33 (gC1q Receptor)

Ariane Neumann[a] Praveen Papareddy[a] Johannes Westman[a]
Ole Hyldegaard[b] Johanna Snäll[c] Anna Norrby-Teglund[c] Heiko Herwald[a]

[a]Division of Infection Medicine, Department of Clinical Sciences, Faculty of Medicine, Lund University, Lund, Sweden; [b]Department of Anaesthesia, Rigshospitalet, Copenhagen, Denmark, and [c]Center for Infectious Medicine, Karolinska Institutet, Karolinska University Hospital, Stockholm, Sweden

Keywords
Neutrophil extracellular traps · Danger-associated molecular pattern molecules · *Streptococcus pyogenes* infection · Innate immunity

Abstract
The formation of neutrophil extracellular traps (NETs) is a host defence mechanism, known to facilitate the entrapment and growth inhibition of many bacterial pathogens. It has been implicated that the translocation of myeloperoxidase (MPO) from neutrophilic granules to the nucleus is crucial to this process. Under disease conditions, however, excessive NET formation can trigger self-destructive complications by releasing pathologic levels of danger-associated molecular pattern molecules (DAMPs). To counteract such devastating immune reactions, the host has to rely on precautions that help circumvent these deleterious effects. Though the induction of DAMP responses has been intensively studied, the mechanisms that are used by the host to down-regulate them are still not understood. In this study, we show that p33 is an endothelial-derived protein that has the ability to annul NET formation. We found that the expression of human p33 is upregulated in endothelial cells upon infections with *Streptococcus pyogenes* bacteria. Using tissue biopsies from a patient with streptococcal necrotising fasciitis, we monitored co-localisation of p33 with MPO. Further in vitro studies revealed that p33 is able to block the formation of DAMP-induced NET formation by inhibiting the enzymatic activity of MPO. Additionally, mice challenged with *S. pyogenes* bacteria demonstrated diminished MPO activity when treated with p33. Together, our results demonstrate that host-derived p33 has an important immunomodulating function that helps to counterbalance an overwhelming DAMP response.

Introduction

Activation of polymorphonuclear cells or neutrophils (PMNs) is one of the first host immune responses to combat invading microbes. To this end, PMNs are equipped with a manifold arsenal of antimicrobial tools including the degranulation of bacteriolytic agents [1], the phagocytosis of pathogens [2], and the formation of neutrophil extracellular traps (NETs) [3]. Within the last decade, this last mechanism has attracted much attention because

Current address of Johannes Westman: Division of Cell Biology, Hospital for Sick Children, Toronto, ON, Canada

KARGER

E-Mail karger@karger.com
www.karger.com/jin

Dr. Ariane Neumann
Division of Infection Medicine, Department of Clinical Sciences
Lund University, BMC, Floor B14
Tornavägen 10, SE–221 84 Lund (Sweden)
E-Mail ariane.neumann@med.lu.se

blood-derived PMNs employ a sophisticated approach to expel web-like structures that can entrap and kill pathogens such as *Staphylococcus aureus*, *Salmonella typhimurium*, and *Shigella flexneri* [3]. Subsequent work by Fuchs et al. [4] showed that PMNs can undergo a special cell death program (NETosis) in order to release their DNA into the surroundings. During this process, antimicrobial agents such as histones, myeloperoxidase (MPO), neutrophil elastase, and the host defence peptide LL-37 become attached to DNA fibres [3, 5, 6] which can further increase the antimicrobial activity of the formed NETs [7].

Though PMN activation and the subsequent generation of NETs are considered important defence mechanisms, recent studies also report that excessive NET formation or impaired NET degradation can be detrimental to the host [8–12]. Along these lines, it has been described that the exaggerated mobilisation of some NET-associated molecules such as LL-37 and extracellular histones can evoke overwhelming inflammatory reactions [13]. Notably, the secretion of LL-37 under pathological conditions [14] can lyse bacterial but also mammalian cell membranes [15], and similar findings have been reported for the histones released from necrotic cells [16]. It therefore seems plausible that the immune system has to take special precautions to counteract the self-destructive activity of these danger-associated molecular patterns (DAMPs). However, the underlying regulative mechanisms behind such down-regulating mechanisms are so far only poorly understood.

Recently, it was reported that p33, also known as the gC1q receptor or p32, is able to inhibit the cytotoxic activity of several antimicrobial peptides, including LL-37 and extracellular histones [17, 18]. Originally, p33 was discovered for its affinity to complement factor C1q [19], but, since then, proteins such as high-molecular-weight kininogen [20], thrombin [21], and lamin B receptor [22] as well as a number of pathogen-associated molecular pattern (PAMP) molecules [23, 24] have also been described as p33 binding partners. The expression of p33 is to be found in many cells types, including lymphocytes, dendritic cells, endothelial cells, and platelets [20, 25, 26]. In these cells, p33 has been detected in various compartments such as the nucleus, mitochondria, cell membrane, and extracellular matrix [27, 28]. The expression of p33 is up-regulated in the endothelial cells by pro-inflammatory stimuli including TNFα, IFNγ, and lipopolysaccharide [29], or under hypoxic conditions [30]. The fact that p33 can protect host cells from a lytic attack by DAMPs such as LL-37 and extracellular histones and that it is up-regulated under pathological conditions points to an important role of the protein in dampening an over-accelerated host response under infectious disease conditions [31]. Thus, p33 is an interesting protein for studying its ability to down-regulate the toxic side effects evoked by the release of DAMPs exceeding pathological levels.

In this study, we investigated the influence of p33 on the DAMP-facilitated NET generation. We found that p33 is up-regulated in endothelial cells upon bacterial challenge. Moreover, our results show that p33 is able to dampen NET formation by binding to and inhibiting the enzymatic activity of MPO, a crucial protein in the neutrophil host defence.

Materials and Methods

Bacterial Strain

Streptococcus pyogenes strain AP1 (40/58; WHO Collaborating Centre for References and Research on Streptococci, Institute of Hygiene and Epidemiology, Prague, Czech Republic) was grown in THY medium at 37°C to mid-log phase. For the infection experiments, the bacteria were washed with PBS and re-suspended in DMEM medium (Gibco) + 10% FCS (Thermo Fisher Scientific [Thermo]) or PBS. For the NET induction experiments, bacteria were heat-inactivated for 15 min at 65°C and stored at –80°C until further use.

Animals

Wild-type C57BL/6 mice (Charles River Laboratories) were housed under standard conditions and fed with laboratory chow. Water and food were given ad libitum. Experiments were performed with 22-week-old male animals and were approved by the local ethics committee, the Malmö-Lund Animal Care Ethics Committee (M138-13).

PMN Isolation and NET Induction

PMNs were isolated from blood donated by healthy donors (approved by the ethics committee at Lund University, Lund, Sweden) as described previously [32]. Briefly, heparinised blood was layered on top of PolymorphPrep™ (Axis-Shield) and centrifuged at 370 *g* for 30 min at room temperature (RT). Neutrophils were re-suspended in HBSS medium with Ca^{2+}/Mg^{2+} (Gibco) and 2×10^5 cells were seeded onto poly-L-lysine-coated (Sigma) glass slides. Samples were incubated for 3 h at 37°C with 5% CO_2 with 5 μM LL-37 (Schafer-N) or 50 μg/mL calf thymus histones (CTHs; Roche) +/– MBP-p33 (333.3 or 100 μg/mL, respectively; purified as described previously [18]). When 25 nM PMA (Sigma) was used, 100 μg/mL p33 was added. *S. pyogenes* AP1 was used at a multiplicity of infection (MOI) of 10. Cells were fixed with a final 4% PFA.

Fluorescence Microscopy

NET structures were visualised using an MPO antibody (Santa Cruz) or a DNA/histone 1 antibody (Millipore). Anti-p33 immune serum (Innovagen AB) and anti-β-actin (Abcam) were used in visualisation experiments of p33. Primary antibodies were incubated for 1 h at RT or overnight at 4°C. AlexaFluor 488A or AlexaFluor 633O (Invitrogen) were added as secondary antibodies for 45 min at RT in the dark. Samples were finally embedded in ProLong®

Gold Antifade Mountant with DAPI (Thermo). For super-resolution analysis, neutrophils were stained with Hoechst33342 (Thermo) for 15 min and embedded in ProLong® Gold Antifade Mountant. Slides were analysed using an Eclipse TE300 fluorescence microscope with a PlanFluor 40X/0.60 NA objective, an Eclipse Ti-E microscope with a PlanFluor λ 60X/1.40 NA oil objective, a confocal A1+ microscope with an APO 60X/Oil λS DIC N2/1.4 NA objective (all by Nikon) or a DeltaVision OMX V4 (GE Healthcare) with an 60x/1.42 NA PlanApo objective (Olympus) and immersion oil with a refraction index of 1.524. Fifty-eight *z*-stacks, 0.125-μm-thick, were used for the displayed images.

Tissue Preparation and Immunostaining

Snap-frozen soft tissue collected from a patient with necrotising fasciitis infected with an *emm*1 *S. pyogenes* strain was cryosectioned, fixed, and stained (essentially as described previously [33], with 2 modifications). Incubation with primary antibodies, anti-MPO (Santa Cruz) and anti-p33 (Innovagen AB) took place overnight at 4°C, and then ProLong® Gold Antifade Mountant with DAPI (Molecular Probes) was added together with the secondary antibodies, AlexaFluor 488 and AlexaFluor 546 (Molecular Probes). A Nikon A1R confocal microscope was used for imaging and image evaluation (Nikon Instruments).

Scanning Electron Microscopy

For the scanning electron microscopy (SEM) analysis, 2×10^6/mL cells were treated with either 25 nM PMA alone or 25 nM PMA + 100 μg/mL p33 for 3 h at 37°C and 5% CO_2. Samples were spun down with 370 *g*, re-suspended in 2.5% glutaraldehyde (Merck) in 15 mM Na-cacodylate (Sigma) and transferred to poly-L-lysine coated titanium slides. After overnight fixation at RT, samples were dehydrated for 1 h and critical-point dried. Finally, samples were coated with 20 nm Au-palladium and analysed using a Phenom ProX desktop scanning electron microscope (PhenomWorld) with an acceleration voltage of 10 kV.

MPO Release and Enzyme Activity Detection

For the measurement of MPO activity, 1×10^5 cells per well were incubated for 3 h at 37°C with 5 μM LL-37, 50 μg/mL CTHs, or *S. pyogenes* (MOI 10 +/– 333.3 or 100 μg/mL p33). After incubation, supernatants were transferred into a new plate (Nunc). Collected air-pouch fluids were handled accordingly. For enzyme activity inhibition, 5 mU/mL of recombinant MPO (Thermo) were incubated +/– 333.3 μg/mL of full p33 or 4.8 μg/mL p33-derived peptides for 30 min at RT; 3′-(p-aminophenyl) fluorescein (Invitrogen) was used as substrate. Fluorescence intensity was measured according to the manufacturer's recommendations at ex/em 485/530 nm.

MPO-p33 ELISA

The interaction of MPO with p33 or p33-derived peptides was tested using an ELISA as described earlier [17]. Briefly, plates (Nunc) were coated overnight at 4°C with 2 μg/mL p33 or 0.48 μg/mL peptide in coating buffer (15.9 mM Na_2CO_3, 30 mM $NaHCO_3$, pH 9.6) and blocked in PBS-Tween for 60 min at 37°C. Subsequently, plates were incubated with 1 μg/mL MPO for 1 h at 37°C. Binding of MPO was detected using an MPO antibody (Santa Cruz) and a (H + L)-HRP conjugated antibody (BioRad) each, at 37°C for 1 h. Stabilised TMB chromogen (Thermo) was used as a substrate. The reaction was terminated with 10% H_2SO_4 and measured at 450 nm.

Western Blot Analysis of p33

EA.hy926 cells were grown to 80% confluency and infected with *S. pyogenes* strain AP1 for 3 h with a MOI of 10. Cells were lysed with RIPA buffer (Thermo) and SDS PAGE was run for 35 min at constant 200 V. Samples were transferred onto PVDF membrane (Millipore) for 30 min at constant 15 V. Membranes were incubated overnight at 4°C with primary antibodies (anti-p33 and anti-β-actin, Abcam). Secondary HRP-conjugated antibody (BioRad) was added for 1 h at RT. Bands were visualised using West Pico chemiluminescent substrate (Thermo).

p33 Transfection and Co-Incubation Experiments

EA.hy926 cells were transfected using 25 nM p33 siRNA (Hs_C1QBP_6) or All Stars Negative Control (Qiagen) using Oligofectamine in OptiMEM medium (Life Technologies). Cells were incubated with the siRNA for 48 h at 37°C and 5% CO_2. PMNs were pre-incubated with 25 nM PMA for 20 min and then added onto the endothelial cells with 1×10^5 cells/mL and co-incubated for another 3 h at 37°C and 5% CO_2. Supernatants were collected and the release of MPO was measured as described above.

Chemotaxis Assay

PMNs were isolated as described above and seeded with 200 μL 2×10^6 cells in the upper compartment of a transwell insert with a pore size of 3.0 μm; 500 μL of 10, 50, or 100 μg/mL p33, or 10 nM fMLP was used as chemo-attractant. HBSS medium was used as a negative control. Following incubation for 1, 2, or 3 h at 37°C, the cells in the lower compartment were counted using a Nikon bright-field microscope with a ×20 bright-field air objective and ImageJ software.

Animal Infection Experiment

Male C57BL/6 mice (aged 22 weeks) were subcutaneously injected with 10^8 CFU/mL *S. pyogenes* AP1 into an air pouch, as described earlier [34]. PBS was used as the vehicle control. After 24 h, 50 μg/mL p33 or PBS was added for an additional 8 h. Air pouches were rinsed with PBS and the fluids were collected. MPO release was analysed as described above. Cell number was determined using a LUNA™ automated cell counter (Logos Biosystems).

Statistical Analysis

Data was analysed by using GraphPad Prism v7.0 (GraphPad Software). Differences between 2 groups were analysed by using a

Fig. 1. Upon bacterial infection, p33 is up-regulated in endothelial cells. **a** Representative fluorescence micrographs of EA.hy926 cells control or infected with *S. pyogenes* strain AP1 after 3 h. DNA, blue; p33, purple; β-actin, green. Scale bar, 10 μm. **b** Western blot of EA.hy926 cell lysates in non-treated and infected cells after 3 h. **c** p33 bands were quantified and normalised to β-actin. **d** Transwell chemotaxis assay. Neutrophils were incubated for 1, 2, and 3 h with 10, 50, and 100 μg/mL p33 and 10 nM fMLP. **e** Total cell count of fluids collected from *S. pyogenes* air-pouch infection. Data represents mean +/– SEM of 3 independent experiments. Ctr, control/non-treated cells; Inf, infected cells. * $p \leq 0.05$, ** $p \leq 0.01$, *** $p \leq 0.001$, **** $p \leq 0.0001$.

(For figure see next page.)

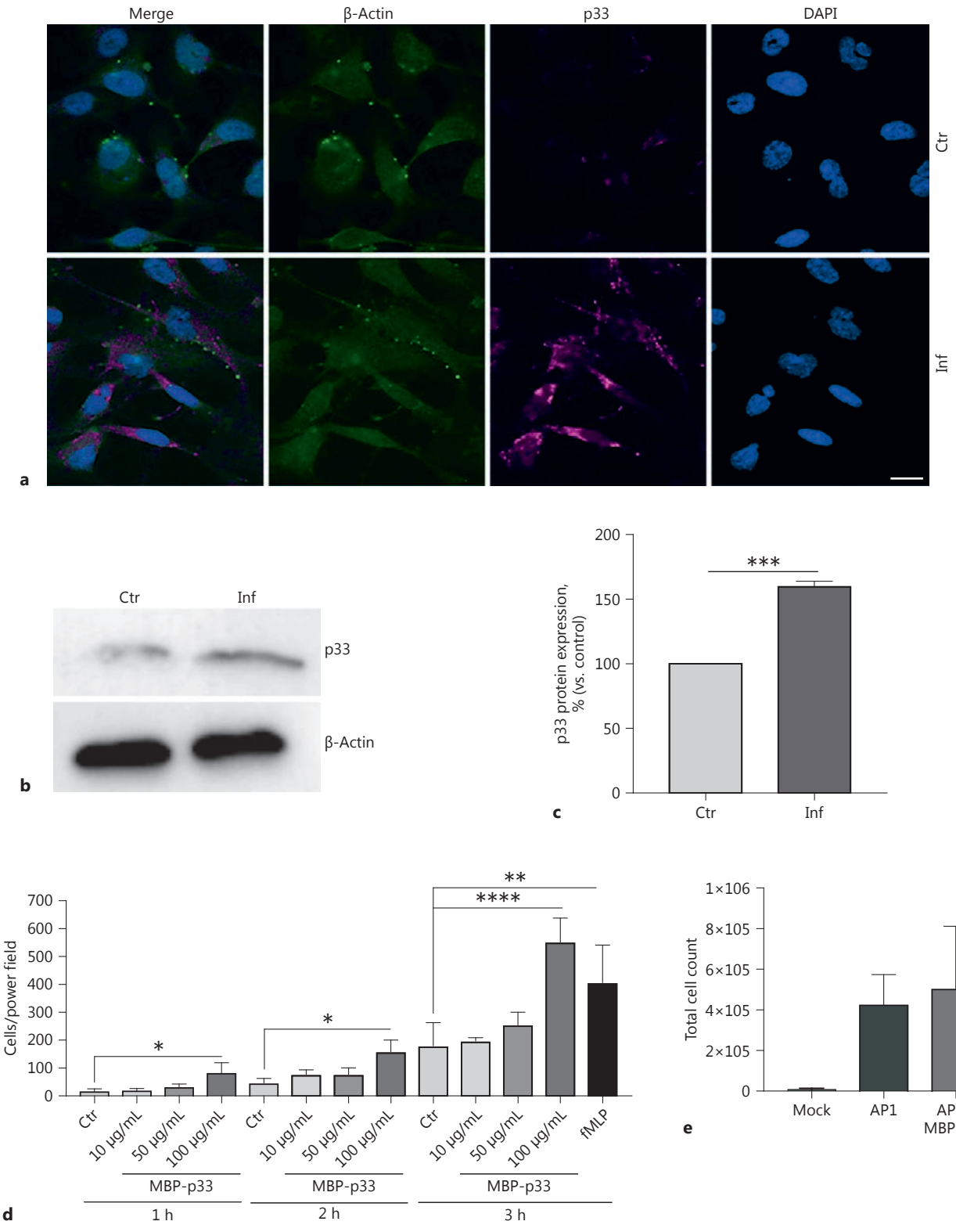
Merge
β-Actin
p33
DAPI
Ctr
Inf
a
Ctr
Inf
p33
β-Actin
b
p33 protein expression, % (vs. control)
200
150
100
50
0
***
Ctr
Inf
c
Cells/power field
700
600
500
400
300
200
100
0
*
*
**
****
Ctr
10 μg/mL
50 μg/mL
100 μg/mL
fMLP
MBP-p33
1 h
2 h
3 h
d
Total cell count
1×106
8×105
6×105
4×105
2×105
0
Mock
AP1
AP1+ MBP-p33
e

1

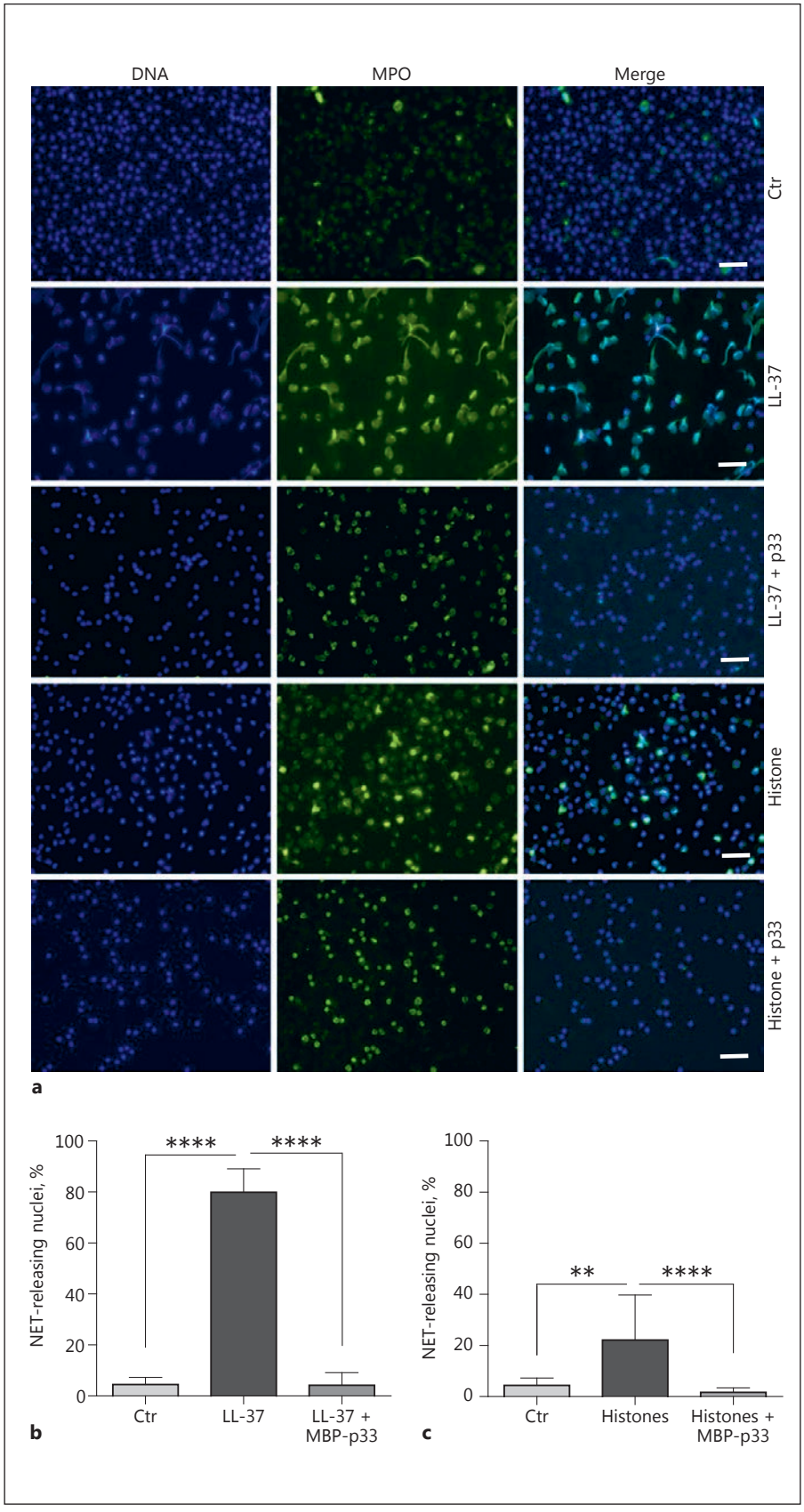

Fig. 2. p33 impairs DAMP-mediated NET release. **a** Representative immuno-fluorescent micrographs display the results shown in **b** and **c**. NET structures were visualised with MPO (green) and DAPI (blue). Scale bar, 50 µm. **b**, **c** Human neutrophils were treated for 3 h with 5 µm LL-37 and 50 µg/ml CTHs, respectively. Recombinant p33 was added simultaneously in a 2:1 ratio. 3 independent experiments +/– SEM. Ctr, control. ** $p \leq 0.01$, **** $p \leq 0.0001$.

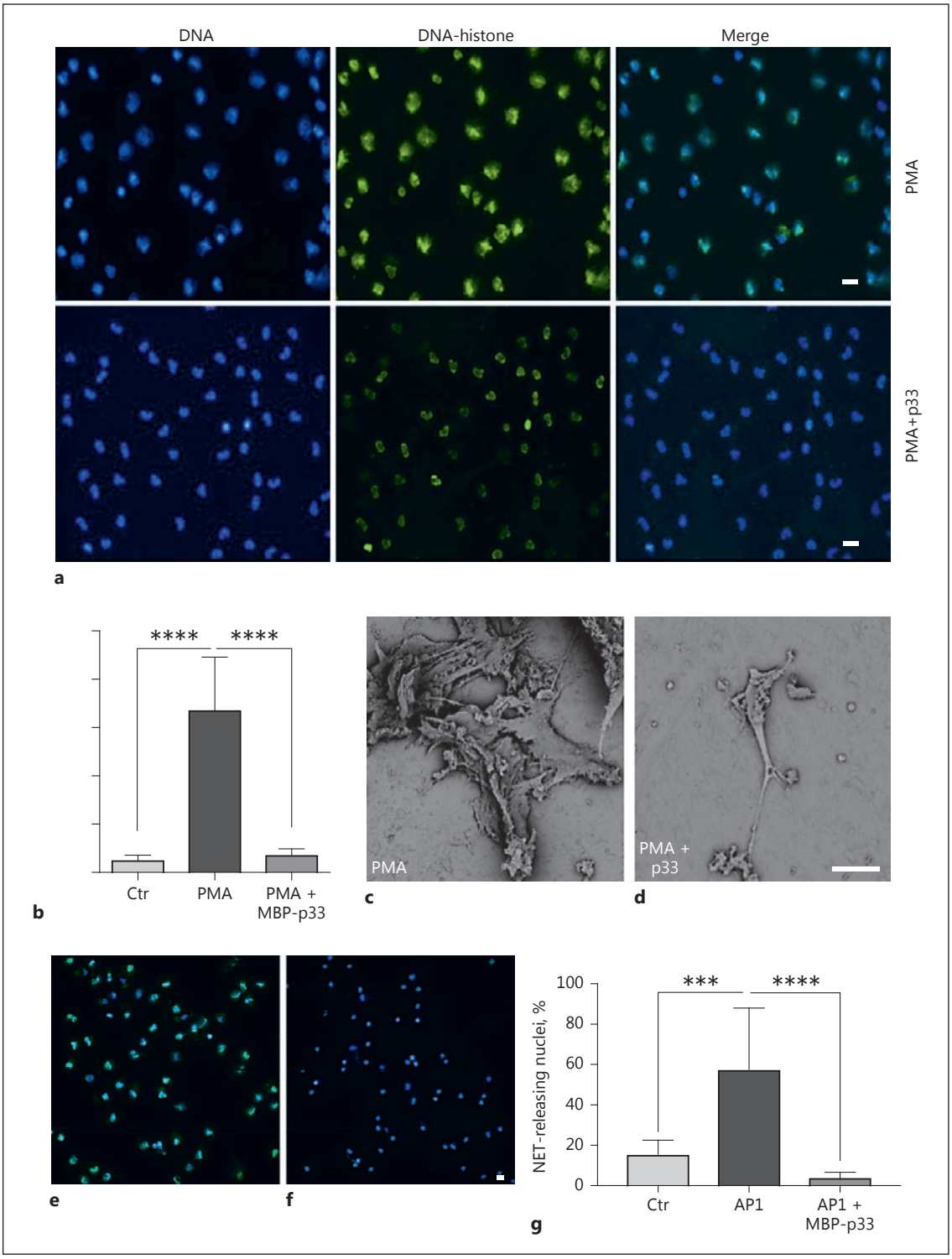

Fig. 3. a Representative fluorescence microscopy images of the PMA-triggered NET release. Histone H1, green; nuclei, blue. Scale bar, 50 µm. **b** Inhibitory effect of 100 µg/mL p33 on human PMNs incubated with 25 nM PMA for 3 h. **c**, **d** Scanning electron micrographs of 25 nM PMA-induced NETs in the presence or absence of 100 µg/mL p33. ×1,850. Scale bar, 30 µm. **e**, **f** Representative fluorescence images of NET formation induced by *S. pyogenes* AP1. Histone H1, green; nuclei, blue. Scale bar, 30 µm. **g** The addition of 100 µg/mL p33 shows significant inhibition of *S. pyogenes*-induced NET release. Data is for 3 independent experiments; unpaired one-tailed Student *t* test +/– SEM. *** $p < 0.001$, **** $p \leq 0.0001$.

paired, one-tailed Student *t* test or 1-way ANOVA with the Bonferroni post hoc test. Significance is indicated as * $p \leq 0.05$, ** $p \leq 0.01$, *** $p \leq 0.001$, and **** $p \leq 0.0001$.

Results

Under Infectious Conditions: p33 Is Up-Regulated and Attracts PMNs

Recent studies have shown that MrgC1qR, the p33 homologue in fresh-water prawns, is significantly elevated upon bacterial challenge [35]. To study whether human p33 is also up-regulated upon infection with gram-positive bacteria, we treated human umbilical vein endothelial EA.hy926 cells (ATCC® CRL-2922™) for 3 h with the *S. pyogenes* AP1 strain. Protein expression under infectious conditions was investigated by employing fluorescence microscopy and Western blot analysis. A clear up-regulation of p33 by fluorescence microscopy (Fig. 1a) was noted in infected cells compared to the uninfected control, and confirmed by Western blot analysis (Fig. 1b, c).

During infection or tissue damage, DAMPs and other cellular components can activate neutrophils and attract them to migrate to the site of bacterial colonisation (review [36]). A cell migration assay revealed that after 1 h of incubation, 100 μg/mL MBP-p33 acts as a chemo-attractant for PMNs in vitro (Fig. 1d). Based on these findings, we decided to use this concentration for further experiments. To investigate this phenotype in an animal model, we infected 22-week-old male C57BL/6 mice with the *S. pyogenes* strain AP1, using an air-pouch model [34]. Subsequently, MBP-p33 was added, before fluids from the air pouch were collected and analysed for infiltrated cell counts. As shown in Figure 1e, the addition of MBP-p33 had a slight impact on the infiltration of total immune cells at the site of infection. Based on these findings, we hypothesised that p33 can modulate the host response under infectious disease conditions.

Administration of p33 Inhibits DAMP- and PMA-Triggered NET Formation

Next, we investigated the effect of p33 on NET formation triggered by DAMPs like LL-37 and histones. These antimicrobial molecules, when excessively released during inflammatory conditions [14] or tissue damage [37, 38], can have a self-destructive impact [39–41]. It has been shown that the interaction of MBP-p33 with LL-37 and histones can abrogate the cytolytic activity of these agents, which in turn helps to counteract endogenous destruction [17, 18]. In addition, it has also been reported that both LL-37 and histones can trigger the release of NETs [32, 42]. To address the hypothesis whether p33 can modulate NET formation, we stimulated human PMNs with LL-37 and CTHs for 3 h in the presence or absence of MBP-p33. Co-incubation of PMNs with 5 μM LL-37 for 3 h led to a greater release of NETs (Fig. 2a, b). Similar findings were recorded when CTHs (50 μg/mL) were used, even though NET formation was less pronounced (Fig. 2a, c). The simultaneous administration of MBP-p33, in a 2:1 ratio to either LL-37 (Fig. 2b) or CTHs (Fig. 2c), almost completely abolished the formation of NETs. We therefore concluded that p33 is involved in the regulation of NET formation triggered by DAMPs like LL-37 and histones. Next, we stimulated human PMNs with 25 nM PMA (a well-described NET inducer [3, 43]) for 3 h, which resulted in a significant release of extracellular DNA fibres. This was significantly diminished by the simultaneous application of 100 μg/mL MBP-p33 (Fig. 3a, b). SEM confirmed this observation. PMA treatment led to extensive, widespread fibrous structures (Fig. 3c) but under the same experimental conditions, co-stimulation with MBP-p33 resulted in less-pronounced NET structures (Fig. 3d).

It has also been reported that NETs are induced by bacteria such as *S. pyogenes* [44]. We wanted to establish whether p33 could affect bacteria-induced NET formation in a manner similar to that described above for DAMPs and PMA. To this end, we incubated PMNs for

Fig. 4. In infected tissue, p33 co-localises with MPO and dampens its release. **a** Representative fluorescence images of neutrophils treated with 25 nM PMA +/– 100 μg/mL p33. DAPI, blue; MPO, green. Scale bar, 10 μm. **b** Representative super-resolution micrograph of p33 (100 μg/mL) with endogenous neutrophil MPO. MPO, green; p33, red; DAPI, blue. Scale bar, 5 μm. **c** Snap-frozen tissue from a patient with necrotising fasciitis caused by an *emm*1 *S. pyogenes* strain was immunostained and assessed for the expression of MPO (green) and p33 (red). Yellow signal indicates co-localisation of p33 and MPO, as shown in the inset. The tissue was counterstained with DAPI to visualise cell nuclei (blue). Scale bar, 20 μm. **d** Effect of siRNA down-regulation of p33 in EA.hy926 cells on MPO release from PMNs after 3 h co-incubation. **e** Lactate dehydrogenase (LDH) assay of 3 h of endothelial cell-PMN co-incubation. ns, not significant. **f**, **g** Measurement of MPO release from PMNs after treatment with 5 μM LL-37 or 50 μg/mL CTHs +/– 333.3 or 100 μg/mL p33, respectively. Data is from 3 independent experiments; unpaired one-tailed Student *t* test +/– SEM. ** $p \leq 0.01$, **** $p \leq 0.0001$.

(For figure see next page.)

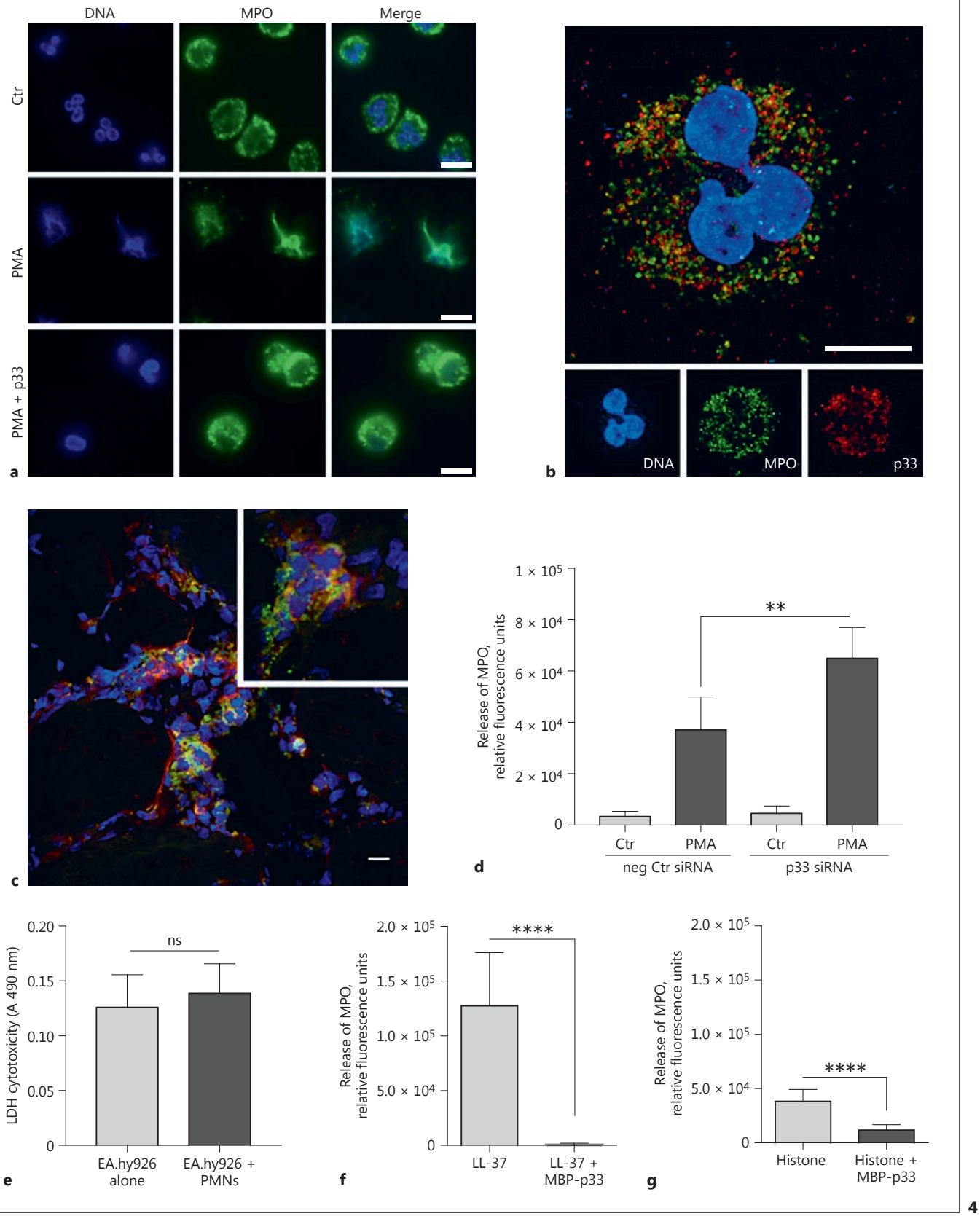
DNA
MPO
Merge
Ctr
PMA
PMA + p33
a
DNA
MPO
p33
b
c
Release of MPO, relative fluorescence units
1 × 10^5
8 × 10^4
6 × 10^4
4 × 10^4
2 × 10^4
0
**
Ctr
PMA
Ctr
PMA
neg Ctr siRNA
p33 siRNA
d
LDH cytotoxicity (A 490 nm)
0.20
0.15
0.10
0.05
0
ns
EA.hy926 alone
EA.hy926 + PMNs
e
Release of MPO, relative fluorescence units
2.0 × 10^5
1.5 × 10^5
1.0 × 10^5
5.0 × 10^4
0
****
LL-37
LL-37 + MBP-p33
f
Release of MPO, relative fluorescence units
2.0 × 10^5
1.5 × 10^5
1.0 × 10^5
5.0 × 10^4
0
****
Histone
Histone + MBP-p33
g

4

3 h with *S. pyogenes* AP1. To prevent immediate degradation of NETs by bacterial nucleases [45], the bacteria were heat-inactivated. As depicted in Figure 3e–g, *S. pyogenes* AP1 triggered NET formation, which was then almost completely abolished by the addition of MBP-p33.

p33 Co-Localises with MPO in Infected Tissue and Interferes with MPO Activity

In the next series of experiments, we wished to unravel the molecular mechanisms employed by p33 to modulate NET formation. Microscopic analysis revealed MPO translocation to the nucleus and chromatin loosening only in the PMA-treated PMNs (Fig. 4a, middle panel), which is in line with reports by others [46]. However, the addition of MBP-p33 to PMA-stimulated PMNs led to a resting of MPO in the granules and condensed chromatin (Fig. 4a, lower panel). This finding was supported by confocal microscopy over a 3-h time course, showing that in PMA-treated PMNs, nuclei start to decondense after 30 min of incubation but that in PMA/p33-treated PMNs, MPO remains in the granules around the nucleus. After 180 min, in the PMA-treated cells, almost all nuclei (80–90%) displayed a mix of chromatin and MPO (online suppl. Fig. 1; for all online suppl. material, see www.karger.com/doi/10.1159/000480386) when compared to PMA/p33-treated cells (approx. 15%). Super-resolution microscopy revealed that externally added MBP-p33 is located in close proximity to the neutrophil protein MPO (Fig. 4b). Consequently, we analysed biopsies from a patient with soft-tissue necrotising fasciitis caused by *emm*1 *S. pyogenes* infection to test whether this interaction has a patho-physiological implication. As shown in Figure 4c, on confocal fluorescence microscopy, we noted co-localisation of endogenous p33 and MPO in severely inflamed tissue.

Next, we sought to investigate whether p33 is able to interfere with the mobilisation of MPO from its granular compartment into the nucleus, which is an established sign of NETosis [3, 47]. Previous work has shown that, upon PMN activation and subsequent ROS production, MPO, in concert with neutrophil elastase, can induce chromatin decondensation and histone degradation in a dose-dependent manner [48]. Based on these reports, we decided to study the effect of endogenous p33 secreted from the endothelial cell line on the release of MPO from PMNs. As a control, we employed EA.hy926 cells in which p33 levels were down-regulated using an siRNA approach. Figure 4d depicts that PMNs incubated with EA.hy926 cells, lacking normal p33 expression, mobilised more MPO than cells treated with negative-control siRNA. To exclude any cytotoxic effect of PMNs on the endothelial cells during co-incubation, we performed a lactate dehydrogenase assay. After a 3-h co-incubation period, we did not measure any increase in lactate dehydrogenase levels compared to endothelial cells alone (Fig. 4e). These results are in line with reports from others [49], and demonstrate that PMNs and their secretion products fail to influence the viability of endothelial cells after 3 h of co-incubation.

Next, we investigated the effect of recombinant MBP-p33 on the release of MPO from PMNs alone, induced by LL-37 and histones. MBP-p33 significantly impaired the degranulation of MPO triggered by LL-37 and by histones (Fig. 4f, g). When measuring the secretion of MPO, we found that PMA stimulation resulted in an increased release of MPO but that the addition of MBP-p33 to PMA-stimulated cells significantly blocked the mobilisation of MPO (Fig. 5a). These findings correlate well with the results obtained from the co-incubation studies (Fig. 4d).

To obtain more structural information about the sequence motif of p33, which is crucial for attenuating the release of MPO from the granules, we included a panel of synthetic peptides derived from p33 [17]. Our data shows that 3 p33-derived peptides (QEP20, TGE20, and FLA20, respectively) significantly blocked the mobilisation of MPO (Fig. 5a). The release of MPO was also measured when PMNs were treated with *S. pyogenes* AP1. Similar to the results obtained with DAMP/PMA-stimulated cells, p33 displayed an inhibitory effect on the se-

Fig. 5. Addition of p33 retains release of MPO from neutrophilic granules. **a** MPO release from PMNs after incubation with 25 nM PMA, 333.3 μg/mL p33, or 4.8 μg/mL p33-derived peptides. **b** Release of MPO from PMNs in response to *S. pyogenes* AP1 in the presence or absence of p33. **c** MPO release of fluids collected after 32 h from *S. pyogenes* AP1-infected air pouch in mice; 3 independent experiments; +/– SEM. **d** p33 and p33-derived peptides were incubated with 5 U/mL MPO. Relative fluorescence units indicate the chlorination activity of MPO, data is from 3 independent experiments, one-way ANOVA +/– SEM. ** $p \leq 0.01$, *** $p \leq 0.001$, **** $p \leq 0.0001$. **e** Production of ROS from PMNs treated with 25 nM PMA +/– 100 μg/mL p33. t_{0-180}, time points in minutes. **f** Binding ability of different p33-derived peptides to MPO compared to full-length p33. **g** 3D structure of p33 using the PDB ID 1P32 [61] in the NCBI iCn3D tool [51]; p33-derived peptides VIK20 (cyan) and TGE20 (magenta) are highlighted.

(For figure see next page.)

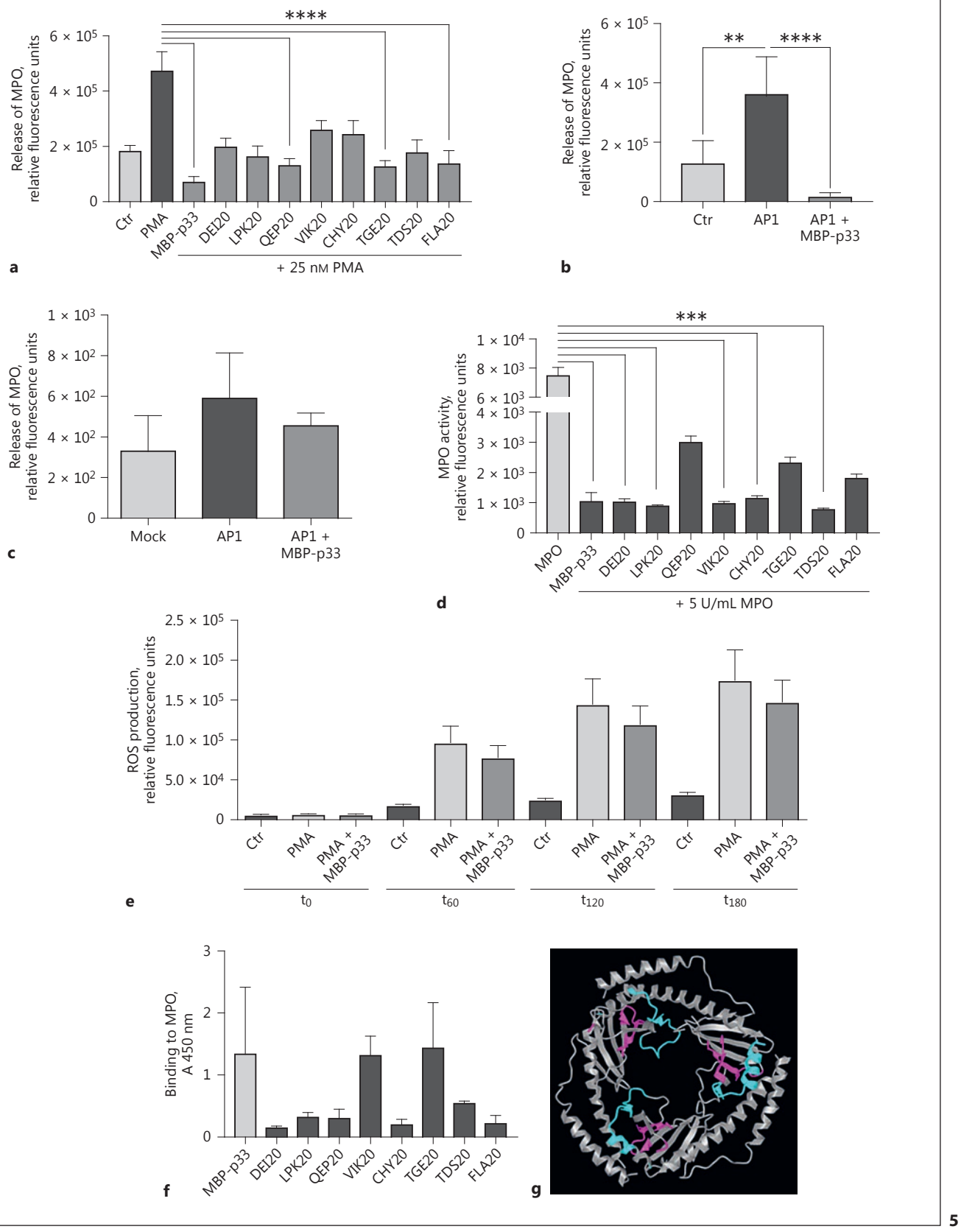
****
Release of MPO, relative fluorescence units
6 × 10^5
4 × 10^5
2 × 10^5
0
Ctr
PMA
MBP-p33
DEI20
LPK20
QEP20
VIK20
CHY20
TGE20
TDS20
FLA20
+ 25 nM PMA
a
**
****
Release of MPO, relative fluorescence units
Ctr
AP1
AP1 + MBP-p33
b
Release of MPO, relative fluorescence units
1 × 10^3
8 × 10^2
6 × 10^2
4 × 10^2
2 × 10^2
Mock
AP1
AP1 + MBP-p33
c
***
MPO activity, relative fluorescence units
1 × 10^4
8 × 10^3
6 × 10^3
4 × 10^3
3 × 10^3
2 × 10^3
1 × 10^3
MPO
MBP-p33
DEI20
LPK20
QEP20
VIK20
CHY20
TGE20
TDS20
FLA20
+ 5 U/mL MPO
d
ROS production, relative fluorescence units
2.5 × 10^5
2.0 × 10^5
1.5 × 10^5
1.0 × 10^5
5.0 × 10^4
Ctr
PMA
PMA + MBP-p33
t0
t60
t120
t180
e
Binding to MPO, A 450 nm
3
2
1
MBP-p33
DEI20
LPK20
QEP20
VIK20
CHY20
TGE20
TDS20
FLA20
f
g

5

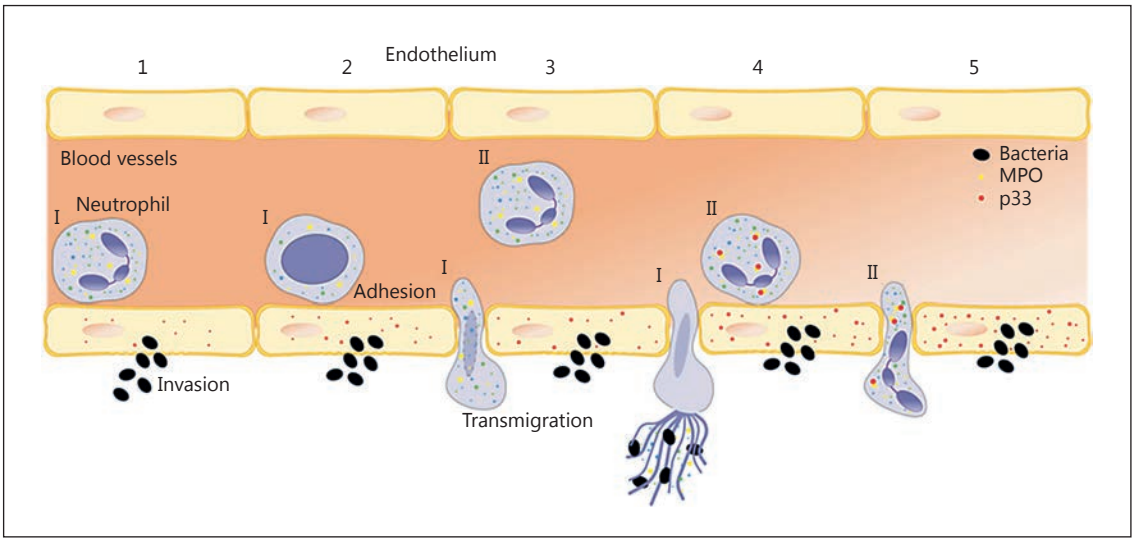

Fig. 6. p33 interaction with MPO in infectious conditions. (I) The first wave of neutrophils (1) adhere to infected endothelium (2). The chromatin loosens, the nuclear membrane disrupts (2) and the neutrophils migrate into the tissue to entrap the invading bacteria (3). (II) Following neutrophils adhere and take up p33 (4), which is up-regulated in the activated endothelium. The neutrophils transmigrate to the site of infection, p33 and MPO interact with each other, and the chromatin remains condensed (5).

cretion of MPO (Fig. 5b). The impact of MBP-p33 on MPO release was also measured in an animal model. In 22-week-old male C57BL/6 mice infected with *S. pyogenes* AP1, we found that the addition of MBP-p33 led to a reduced mobilisation of MPO into the air pouch when challenged with the bacteria (Fig. 5c). Next, we focused on the effect of p33 and p33-derived peptides on the enzyme activity of recombinant MPO. Figure 5d depicts strong competitive enzyme inhibition by MBP-p33, confirming our hypothesis that this protein can block the induction of NET via enzyme inhibition (Fig. 5d). In addition to p33, DEI20, LPK20, VIK20, CHY20, and TDS20 also significantly impair the activity of MPO (Fig. 5d). Active MPO enzyme plays an important, but not solitary part in the production of reactive oxygen species (ROS [50]). We thus tested the influence of p33 on ROS production in PMA-stimulated PMNs over time. As shown in Figure 5e, the production of ROS was impaired by the addition of 100 μg/mL of MBP-p33. Finally, we employed an indirect ELISA to test whether MBP-p33 or p33-derived peptides can bind to MPO. As shown in Figure 5f, direct interaction of MBP-p33 to MPO was detected, and the p33-derived peptides, VIK20 and TGE20, displayed a strong affinity for MPO comparable to the full-length protein. Using the Web-based iCn3D structure viewer [51], the structure of p33 was visualised (Fig. 5g). When looking at the interaction sites of p33 with MPO, it appears that peptides binding to (TGE20) or interfering with MPO enzyme activity (VIK20) are clustered, and located in the inside of the doughnut-shaped trimer (Fig. 5g). This data suggests that p33 interferes with the release of NETs due to the competitive inhibition of MPO enzyme activity. It provides new insights into the role of the multi-ligand protein p33 in innate immunity.

Discussion

This study provides a novel insight into how p33 can modulate the generation of NETs. The release of NETs has been described as an immune response of the host to inflammation and infection [52]. However, in recent years, evidence has accumulated that excessive NET formation and the impaired degradation of the fibre-like structures is correlated to pathological conditions such as sepsis [53] and cell damage [54]. DAMPs, like LL-37 and histones, are cationic, antimicrobial components that are found entangled in the fibrous NET meshwork, and eventually cause considerable damage to the host [39, 40]. Our data shows that MBP-p33 can dampen the formation of NETs triggered by endogenous DAMPs, LL-37, and histones as well as by chemical stimuli, e.g., PMA.

The multi-ligand protein p33 can be detected on cell surfaces and in mitochondria [55, 56]. Previous work has shown that p33 is up-regulated by a variety of pro-inflammatory factors including interferons [29], suggesting that the protein has important functions during infections. As a proof of concept, we infected human umbilical vein endothelial cells EA.hy926 for 3 h with *S. pyogenes*, which led to an up-regulation of p33 as detected by fluorescence microscopy and Western blot analysis. These findings are in good correlation with earlier reports of increased p33 levels under inflammatory condition [30]. Having shown that p33 is up-regulated under infectious conditions in human endothelial cells, we next explored this in infected patients. To this end, we analysed tissue biopsies from a patient with severe *S. pyogenes* soft-tissue infections, which revealed the presence of p33 and MPO at the infected site, as well as co-localisation of the factors.

To unravel the role of p33 in regulating NETosis, a series of experiments were undertaken. Immunofluorescence microscopy revealed that the administration of p33 to PMA-stimulated PMNs results in the persistence of MPO in the granules, which did not mix with the still intact, not yet de-condensed chromatin. In addition, a co-incubation model of endothelial cells with neutrophils revealed increased MPO release when p33 was down-regulated with specific siRNA. For an in vivo proof, MPO release was followed in a mouse model, where *S. pyogenes* bacteria were injected subcutaneously into an air pouch. Here, we also noted a reduced mobilisation of MPO after the administration of MBP-p33 into the air pouch.

It has been suggested that the active MPO enzyme might be important for chromatin breakdown and subsequent NET formation [48, 57]. Our data show that the co-incubation of PMNs with MBP-p33 and its derived peptides resulted in the reduced release of MPO and blocked its enzyme activity. Chemical inhibition of MPO by aminobenzoic acid hydrazide (4-ABAH), which reduced enzyme activity irreversibly by 23% [58], had no effect on chromatin de-condensation [48], but did result in a decrease of NET formation [59]. We therefore speculated that a more physiological inhibitor like the endothelial protein p33 could indeed affect the chromatin de-condensation that is necessary to perform NET formation. This led us to conclude that our findings are of importance also under infectious disease conditions. Excess activation of PMNs by DAMPs or bacteria like *S. pyogenes* and the subsequent release of granular enzymes such as MPO at the site of infection can limit the repair of injury (review [36]) and boost the pathological conditions seen under sepsis or respiratory distress conditions [60]. Additionally, since MPO plays a crucial role in the production of ROS, which can have destructive effects on inflamed tissue, a diminished release of MPO could be beneficial to the host. Thus, our study adds new insights into how the delicate balance of an overwhelming immune response is regulated by endogenous proteins like p33 (Fig. 6). Future studies are needed to further elucidate a possible role of p33 as an effective therapeutic target to attenuate overwhelming PMN-evoked inflammatory responses.

Acknowledgment

The authors would like to thank Maria Baumgarten for excellent technical assistance with the SEM experiments and Dr. Tirthankar Mohanty for helpful discussions.

Disclosure Statement

The authors declare no competing financial interests.

Funding Sources

This work was supported by a scholarship from the Wennergren Foundation (A.N). Further support came from the Alfred Österlund Foundation, the Knut and Alice Wallenberg Foundation [KAW 2011.0037], the Ragnar Söderberg Foundation, the Medical Faculty, Lund University, the Swedish Foundation for Strategic Research [K2014-56X-13413-15-3], and the Swedish Research Council (http://www.vr.se/) [2013-2438]. The funders had no role in study design, data collection and analysis, the decision to publish, or the preparation of the manuscript.

Author Contributions

A.N. designed the study, performed the experiments, analysed the data, and wrote the manuscript. P.P. performed the animal infection experiments. J.W. performed the ELISA experiment. O.H. collected the NSTI biopsy samples. J.S. and A.N.-T. performed the NSTI tissue sectioning and staining. H.H. advised and wrote the manuscript.

References

1 Lehrer RI, Ganz T: Antimicrobial peptides in mammalian and insect host defence. Curr Opin Immunol 1999;11:23–27.
2 Metschnikoff E: Lecture on phagocytosis and immunity. BMJ 1891;1:213–217.
3 Brinkmann V, Reichard U, Goosmann C, Fauler B, Uhlemann Y, Weiss DS, Weinrauch Y, Zychlinsky A: Neutrophil extracellular traps kill bacteria. Science 2004;303:1532–1535.

4 Fuchs TA, Abed U, Goosmann C, Hurwitz R, Schulze I, Wahn V, Weinrauch Y, Brinkmann V, Zychlinsky A: Novel cell death program leads to neutrophil extracellular traps. J Cell Biol 2007;176:231–241.
5 Papayannopoulos V, Zychlinsky A: NETs: a new strategy for using old weapons. Trends Immunol 2009;30:513–521.
6 von Kockritz-Blickwede M, Nizet V: Innate immunity turned inside-out: antimicrobial defense by phagocyte extracellular traps. J Mol Med (Berl) 2009;87:775–783.
7 Gray RD, McCullagh BN, McCray PB: NETs and CF lung disease: current status and future prospects. Antibiotics 2015;4:62–75.
8 Hakkim A, Furnrohr BG, Amann K, Laube B, Abed UA, Brinkmann V, Herrmann M, Voll RE, Zychlinsky A: Impairment of neutrophil extracellular trap degradation is associated with lupus nephritis. Proc Natl Acad Sci USA 2010;107:9813–9818.
9 Lande R, Ganguly D, Facchinetti V, Frasca L, Conrad C, Gregorio J, Meller S, Chamilos G, Sebasigari R, Riccieri V, Bassett R, Amuro H, Fukuhara S, Ito T, Liu YJ, Gilliet M: Neutrophils activate plasmacytoid dendritic cells by releasing self-DNA-peptide complexes in systemic lupus erythematosus. Sci Transl Med 2011;3:73ra19.
10 Garcia-Romo GS, Caielli S, Vega B, Connolly J, Allantaz F, Xu Z, Punaro M, Baisch J, Guiducci C, Coffman RL, Barrat FJ, Banchereau J, Pascual V: Netting neutrophils are major inducers of type I IFN production in pediatric systemic lupus erythematosus. Sci Transl Med 2011;3:73ra20.
11 Manzenreiter R, Kienberger F, Marcos V, Schilcher K, Krautgartner WD, Obermayer A, Huml M, Stoiber W, Hector A, Griese M, Hannig M, Studnicka M, Vitkov L, Hartl D: Ultrastructural characterization of cystic fibrosis sputum using atomic force and scanning electron microscopy. J Cyst Fibros 2012;11:84–92.
12 Leffler J, Prohaszka Z, Mikes B, Sinkovits G, Ciacma K, Farkas P, Reti M, Kelen K, Reusz GS, Szabo AJ, Martin M, Blom AM: Decreased neutrophil extracellular trap degradation in Shiga toxin-associated haemolytic uraemic syndrome. J Innate Immun 2017;9:12–21.
13 Srikrishna G, Freeze HH: Endogenous damage-associated molecular pattern molecules at the crossroads of inflammation and cancer. Neoplasia 2009;11:615–628.
14 Frohm M, Agerberth B, Ahangari G, Stahle-Backdahl M, Liden S, Wigzell H, Gudmundsson GH: The expression of the gene coding for the antibacterial peptide LL-37 is induced in human keratinocytes during inflammatory disorders. J Biol Chem 1997;272:15258–15263.
15 Johansson J, Gudmundsson GH, Rottenberg ME, Berndt KD, Agerberth B: Conformation-dependent antibacterial activity of the naturally occurring human peptide LL-37. J Biol Chem 1998;273:3718–3724.
16 Kawasaki H, Iwamuro S: Potential roles of histones in host defense as antimicrobial agents. Infect Disord Drug Targets 2008;8:195–205.
17 Westman J, Hansen FC, Olin AI, Morgelin M, Schmidtchen A, Herwald H: p33 (gC1q receptor) prevents cell damage by blocking the cytolytic activity of antimicrobial peptides. J Immunol 2013;191:5714–5721.
18 Westman J, Smeds E, Johansson L, Morgelin M, Olin AI, Malmstrom E, Linder A, Herwald H: Treatment with p33 curtails morbidity and mortality in a histone-induced murine shock model. J Innate Immun 2014;6:819–830.
19 Ghebrehiwet B, Peerschke EI: Structure and function of gC1q-R: a multiligand binding cellular protein. Immunobiology 1998;199:225–238.
20 Herwald H, Dedio J, Kellner R, Loos M, Muller-Esterl W: Isolation and characterization of the kininogen-binding protein p33 from endothelial cells. Identity with the gC1q receptor. J Biol Chem 1996;271:13040–13047.
21 Ghebrehiwet B, Peerschke EI: Role of C1q and C1q receptors in the pathogenesis of systemic lupus erythematosus. Curr Dir Autoimmun 2004;7:87–97.
22 Nikolakaki E, Simos G, Georgatos SD, Giannakouros T: A nuclear envelope-associated kinase phosphorylates arginine-serine motifs and modulates interactions between the lamin B receptor and other nuclear proteins. J Biol Chem 1996;271:8365–8372.
23 Braun L, Ghebrehiwet B, Cossart P: gC1q-R/p32, a C1q-binding protein, is a receptor for the InlB invasion protein of *Listeria monocytogenes*. EMBO J 2000;19:1458–1466.
24 Nguyen T, Ghebrehiwet B, Peerschke EI: *Staphylococcus aureus* protein A recognizes platelet gC1qR/p33: a novel mechanism for staphylococcal interactions with platelets. Infect Immun 2000;68:2061–2068.
25 Choi Y, Kwon YC, Kim SI, Park JM, Lee KH, Ahn BY: A hantavirus causing hemorrhagic fever with renal syndrome requires gC1qR/p32 for efficient cell binding and infection. Virology 2008;381:178–183.
26 Peerschke EI, Murphy TK, Ghebrehiwet B: Activation-dependent surface expression of gC1qR/p33 on human blood platelets. Thromb Haemost 2003;89:331–339.
27 Ghebrehiwet B, Lim BL, Peerschke EI, Willis AC, Reid KB: Isolation, cDNA cloning, and overexpression of a 33-kD cell surface glycoprotein that binds to the globular "heads" of C1q. J Exp Med 1994;179:1809–1821.
28 Peterson KL, Zhang W, Lu PD, Keilbaugh SA, Peerschke EI, Ghebrehiwet B: The C1q-binding cell membrane proteins cC1q-R and gC1q-R are released from activated cells: subcellular distribution and immunochemical characterization. Clin Immunol Immunopathol 1997;84:17–26.
29 Guo WX, Ghebrehiwet B, Weksler B, Schweitzer K, Peerschke EI: Up-regulation of endothelial cell binding proteins/receptors for complement component C1q by inflammatory cytokines. J Lab Clin Med 1999;133:541–550.
30 Fogal V, Zhang L, Krajewski S, Ruoslahti E: Mitochondrial/cell-surface protein p32/gC1qR as a molecular target in tumor cells and tumor stroma. Cancer Res 2008;68:7210–7218.
31 Yadav G, Prasad RL, Jha BK, Rai V, Bhakuni V, Datta K: Evidence for inhibitory interaction of hyaluronan-binding protein 1 (HABP1/p32/gC1qR) with *Streptococcus pneumoniae* hyaluronidase. J Biol Chem 2009;284:3897–3905.
32 Neumann A, Berends ET, Nerlich A, Molhoek EM, Gallo RL, Meerloo T, Nizet V, Naim HY, von Kockritz-Blickwede M: The antimicrobial peptide LL-37 facilitates the formation of neutrophil extracellular traps. Biochem J 2014;464:3–11.
33 Snall J, Linner A, Uhlmann J, Siemens N, Ibold H, Janos M, Linder A, Kreikemeyer B, Herwald H, Johansson L, Norrby-Teglund A: Differential neutrophil responses to bacterial stimuli: streptococcal strains are potent inducers of heparin-binding protein and resistin-release. Sci Rep 2016;6:21288.
34 Shannon O, Rydengard V, Schmidtchen A, Morgelin M, Alm P, Sorensen OE, Bjorck L: Histidine-rich glycoprotein promotes bacterial entrapment in clots and decreases mortality in a mouse model of sepsis. Blood 2010;116:2365–2372.
35 Ye T, Huang X, Wang XW, Shi YR, Hui KM, Ren Q: Characterization of a gC1qR from the giant freshwater prawn, *Macrobrachium rosenbergii*. Fish Shellfish Immunol 2015;43:200–208.
36 de Oliveira S, Rosowski EE, Huttenlocher A: Neutrophil migration in infection and wound repair: going forward in reverse. Nat Rev Immunol 2016;16:378–391.
37 Fuchs TA, Bhandari AA, Wagner DD: Histones induce rapid and profound thrombocytopenia in mice. Blood 2011;118:3708–3714.
38 Kutcher ME, Xu J, Vilardi RF, Ho C, Esmon CT, Cohen MJ: Extracellular histone release in response to traumatic injury: implications for a compensatory role of activated protein C. J Trauma Acute Care Surg 2012;73:1389–1394.
39 Ciornei CD, Sigurdardottir T, Schmidtchen A, Bodelsson M: Antimicrobial and chemoattractant activity, lipopolysaccharide neutralization, cytotoxicity, and inhibition by serum of analogs of human cathelicidin LL-37. Antimicrob Agents Chemother 2005;49:2845–2850.
40 Singh RK, Liang D, Gajjalaiahvari UR, Kabbaj MH, Paik J, Gunjan A: Excess histone levels mediate cytotoxicity via multiple mechanisms. Cell Cycle 2010;9:4236–4244.

41 Xu J, Zhang X, Pelayo R, Monestier M, Ammollo CT, Semeraro F, Taylor FB, Esmon NL, Lupu F, Esmon CT: Extracellular histones are major mediators of death in sepsis. Nat Med 2009;15:1318–1321.
42 Abrams ST, Zhang N, Manson J, Liu T, Dart C, Baluwa F, Wang SS, Brohi K, Kipar A, Yu W, Wang G, Toh CH: Circulating histones are mediators of trauma-associated lung injury. Am J Respir Crit Care Med 2013;187:160–169.
43 Mohanty T, Sjogren J, Kahn F, Abu-Humaidan AH, Fisker N, Assing K, Morgelin M, Bengtsson AA, Borregaard N, Sorensen OE: A novel mechanism for NETosis provides antimicrobial defense at the oral mucosa. Blood 2015;126:2128–2137.
44 Li P, Li M, Lindberg MR, Kennett MJ, Xiong N, Wang Y: PAD4 is essential for antibacterial innate immunity mediated by neutrophil extracellular traps. J Exp Med 2010;207:1853–1862.
45 Sumby P, Barbian KD, Gardner DJ, Whitney AR, Welty DM, Long RD, Bailey JR, Parnell MJ, Hoe NP, Adams GG, Deleo FR, Musser JM: Extracellular deoxyribonuclease made by group A *Streptococcus* assists pathogenesis by enhancing evasion of the innate immune response. Proc Natl Acad Sci USA 2005;102:1679–1684.
46 Brinkmann V, Zychlinsky A: Beneficial suicide: why neutrophils die to make NETs. Nat Rev Microbiol 2007;5:577–582.
47 Urban CF, Ermert D, Schmid M, Abu-Abed U, Goosmann C, Nacken W, Brinkmann V, Jungblut PR, Zychlinsky A: Neutrophil extracellular traps contain calprotectin, a cytosolic protein complex involved in host defense against *Candida albicans*. PLoS Pathog 2009;5:e1000639.
48 Papayannopoulos V, Metzler KD, Hakkim A, Zychlinsky A: Neutrophil elastase and myeloperoxidase regulate the formation of neutrophil extracellular traps. J Cell Biol 2010;191:677–691.
49 Gupta AK, Joshi MB, Philippova M, Erne P, Hasler P, Hahn S, Resink TJ: Activated endothelial cells induce neutrophil extracellular traps and are susceptible to NETosis-mediated cell death. FEBS Lett 2010;584:3193–3197.
50 Spickett CM, Jerlich A, Panasenko OM, Arnhold J, Pitt AR, Stelmaszynska T, Schaur RJ: The reactions of hypochlorous acid, the reactive oxygen species produced by myeloperoxidase, with lipids. Acta Biochim Pol 2000;47:889–899.
51 Wang Y, Geer LY, Chappey C, Kans JA, Bryant SH: Cn3D: sequence and structure views for Entrez. Trends Biochem Sci 2000;25:300–302.
52 Goldmann O, Medina E: The expanding world of extracellular traps: not only neutrophils but much more. Front Immunol 2013;3:420.
53 Clark SR, Ma AC, Tavener SA, McDonald B, Goodarzi Z, Kelly MM, Patel KD, Chakrabarti S, McAvoy E, Sinclair GD, Keys EM, Allen-Vercoe E, Devinney R, Doig CJ, Green FH, Kubes P: Platelet TLR4 activates neutrophil extracellular traps to ensnare bacteria in septic blood. Nat Med 2007;13:463–469.
54 Saffarzadeh M, Juenemann C, Queisser MA, Lochnit G, Barreto G, Galuska SP, Lohmeyer J, Preissner KT: Neutrophil extracellular traps directly induce epithelial and endothelial cell death: a predominant role of histones. PLoS One 2012;7:e32366.
55 Soltys BJ, Kang D, Gupta RS: Localization of P32 protein (gC1q-R) in mitochondria and at specific extramitochondrial locations in normal tissues. Histochem Cell Biol 2000;114:245–255.
56 Waggoner SN, Cruise MW, Kassel R, Hahn YS: gC1q receptor ligation selectively downregulates human IL-12 production through activation of the phosphoinositide 3-kinase pathway. J Immunol 2005;175:4706–4714.
57 Parker H, Dragunow M, Hampton MB, Kettle AJ, Winterbourn CC: Requirements for NADPH oxidase and myeloperoxidase in neutrophil extracellular trap formation differ depending on the stimulus. J Leukoc Biol 2012;92:841–849.
58 Kettle AJ, Gedye CA, Winterbourn CC: Mechanism of inactivation of myeloperoxidase by 4-aminobenzoic acid hydrazide. Biochem J 1997;321:503–508.
59 Metzler KD, Fuchs TA, Nauseef WM, Reumaux D, Roesler J, Schulze I, Wahn V, Papayannopoulos V, Zychlinsky A: Myeloperoxidase is required for neutrophil extracellular trap formation: implications for innate immunity. Blood 2011;117:953–959.
60 Lacy P: Mechanisms of degranulation in neutrophils. Allergy Asthma Clin Immunol 2006;2:98–108.
61 Jiang J, Zhang Y, Krainer AR, Xu RM: Crystal structure of human p32, a doughnut-shaped acidic mitochondrial matrix protein. Proc Natl Acad Sci USA 1999;96:3572–3577.